

Mathematical Modelling of Avascular Tumour Growth with Irradiation

Andy Nong (20618952)
Vincent Shadbolt (20617236)

University of Waterloo
Faculty of Science
Department of Biology Cross-Listed with Applied Mathematics

AMATH/BIOL 382
Brian Ingalls
April 12, 2018

Abstract

Cancer is a torturous group of diseases that affects the lives of people all over the world. Patients and caregivers alike suffer on a daily basis and will continue to do so should research not be furthered. Thus, studying cancer's development and behaviour is invaluable towards improving the quality of life of patients, family members, and clinicians as a whole. Cancerous tumours in particular go through a gestation period known as avascular growth: a biological phenomenon that can be modeled with standard diffusion equation models. Sherratt-Chaplain then fabricated a more detailed model, which utilizes partial differential equations of cell concentrations and growth changing factors such as mitosis, quiescence, necrosis and nutrient supply. This model was recreated and parameters from past experiments conducted by Keng-Cheng Ang were employed to confirm growth patterns. The model was then expanded upon to account for irradiation of the diseased site; allowing for the discussion of optimal radiation treatment intervals. As most treatment methods rarely take into account dynamic growth or inherent response of the tumour, treatment could be amended on a per-patient basis with an overall reduction in recovery time and increased patient quality of life.

1 Introduction

Cancer is one of the leading causes of death for many countries around the globe; including Canada where it is responsible for more than 30% of all casualties within the country [1]. Due to this high mortality rate, it has become one of the largest fields of study in the medical industry and accounts for millions of dollars yearly. Clearly defined, cancer is a group of diseases whereby abnormal cells rapidly and uncontrollably divide, gradually invading surrounding body tissue - a clinical process known as metastasizing [1]. Under normal circumstances, healthy cells in the body go through controlled life stages comprised of growth, division, and death. However, there are times where a cell deviates from this controlled manner due to failed apoptosis which results in unregulated growth and division as to form a lump or mass called a tumour. Such tumours can be defined as either benign or malignant, with the latter of the two containing the cancerous cells that can undergo metastasis as previously described. In the case where multiple malignant tumours are present, they can be classified as the original tumour and its spread derivatives known as metastases.

The study of such tumours' growth has been recorded in experiment whereby they were grown *in vitro*, or in a glass petri dish with a nutrient rich medium [4]. The tumours were observed to be growing as a tiny spheroid that was only several millimetres thick in diameter. As seen in **Figure 1**, the tumour spheroid is made up of multiple tiers of different cells. This can be explained as an initial ball of proliferating, or rapidly dividing, cells that expands outward. As the cells at the center of this mass begin receiving less nutrients, they undergo a process known as quiescence and become quiescent cells as a result. Quiescent cells are living cell that are not currently dividing due to lack of nutrients, but with reintroduction, can recover such ability. While outward growth continues, quiescent cells at the center of the tumour undergo

necrosis due to severe nutrient deficiency and form the necrotic core of the tumour. The necrotic core is incapable of division or motility regardless of any nutrient influx.

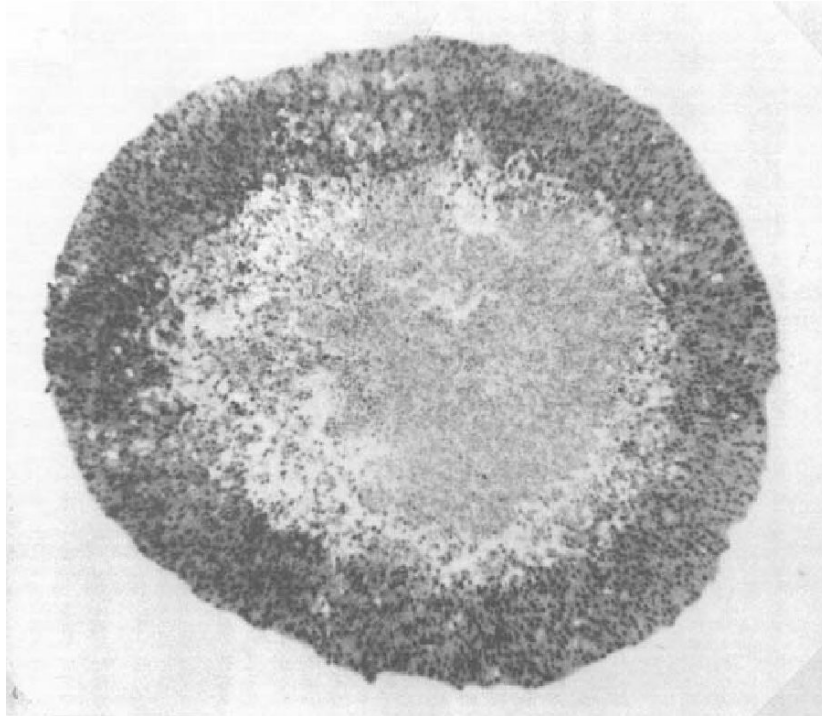


Figure 1: Illustration of avascular tumour with dark outer layer of proliferating cells, inner white layer of quiescent cells, and grey necrotic core; 1.4 mm in diameter [4].

During the early stages of tumour spheroid development, it goes through a gestation period of avascular growth. Here, it has yet to form an internal circulatory structure of blood vessels and thus grows explicitly on external nutrient concentrations [4]. This paper will focus on modelling tumour growth during this stage and will not account for already vascularized masses.

2 Sherratt-Chaplain Model

Modelling tumours with differential equations is a fundamental method that is a critical to cancer research and there is a history of modelling avascular tumour growth in the past century under various approaches such as those presented by Adam and Greenspan [2], [3]. The model employed in this paper is that of Sherratt-Chaplain who published their findings in 2001. Despite being published at the beginning of the 21st century, the model is the most modern and experimentally founded. It incorporates the three different cell types as continuous cell densities on a positive number line, the cell motility, and the nutrient supply *in vivo*, or in the body; providing a more realistic scenario for avascular tumour growth [4]. Note that any deviations made from this model are noted further in the paper.

2.1 The Model

The cell densities of proliferating, quiescent, and necrotic cells will be respectively denoted as $p(x,t)$, $q(x,t)$, and $n(x,t)$ where x represents the one dimensional spatial coordinate and t represents time. A diagram for this model is depicted below in **Figure 2**.

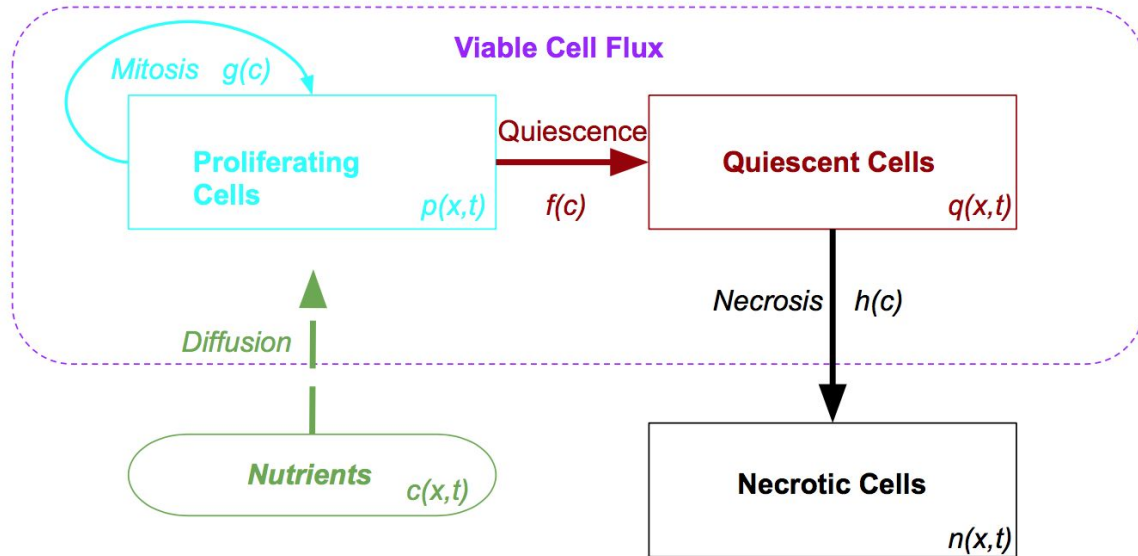


Figure 2: Sherratt-Chaplain Model Diagram of Avascular Tumour Growth

As previously mentioned, the model incorporates cell motility which are represented by movement terms below for proliferating and quiescent cells respectively.

$$\frac{\partial}{\partial x} \left(\frac{p}{p+q} \frac{\partial(p+q)}{\partial x} \right) \quad \text{and} \quad \frac{\partial}{\partial x} \left(\frac{q}{p+q} \frac{\partial(p+q)}{\partial x} \right)$$

These cell motility terms are based off the concept that “the presence of a cell of one type limits the movement of a cell of the other type from moving” [4] known as contact inhibition of migration. They are derived under the safe assumption that proliferating and quiescent cells have equal motility and that the overall viable cell flux is given by $\frac{\partial}{\partial x}(p+q)$. Note that necrotic cells do not have a movement term because they are non-living and thus non-motile. Additionally, the use of a nutrient supply, $c(x,t)$, affects the rates of cellular conversion between proliferating, quiescent, and necrotic as to get the following reduced model equations.

$$\frac{dp}{dt} = \frac{\partial}{\partial x} \left(\frac{p}{p+q} \frac{\partial(p+q)}{\partial x} \right) + g(c)p(1-p-q-n) - f(c)p \quad (1)$$

$$\frac{dq}{dt} = \frac{\partial}{\partial x} \left(\frac{q}{p+q} \frac{\partial(p+q)}{\partial x} \right) + f(c)p - h(c)q \quad (2)$$

$$\frac{\partial n}{\partial t} = h(c)q \quad (3)$$

$$c = \frac{c_0 \gamma}{\gamma - p_i^j} [(1 - \alpha(p+q+n))] \quad (4)$$

In this model the value of '1' in equation 1 describes the closely compacted population of cells within the tumour, alpha, α , in equation 4 represents the buffer between the cells and the external nutrients whereby a lower value corresponds to increased nutrient access, and gamma, γ , represents the in vivo conditions surrounding the tumour. Note that both alpha and gamma are dimensionless parameters.

Using forward differencing for time and central differencing for space on the reduced model equations, the following partial differential equations (PDEs) are obtained:

$$p_i^{j+1} = p_i^j + \Delta t [u_i^j + g(c_i^j)p_i^j(1-p_i^j-q_i^j-n_i^j) - f(c_i^j)p_i^j] \quad (5)$$

$$q_i^{j+1} = q_i^j + \Delta t [v_i^j + f(c_i^j)p_i^j - h(c_i^j)q_i^j] \quad (6)$$

$$n_i^{j+1} = n_i^j + \Delta t [h(c_i^j)q_i^j] \quad (7)$$

$$c_i^j = \frac{\gamma}{\gamma - p_i^j} [(1 - \alpha(p_i^j + q_i^j + n_i^j))] \quad (8)$$

where

$$u_i^j = \frac{(p_{i+1}^j - p_{i-1}^j)r_i^j(r_{i+1}^j - r_{i-1}^j) + 4p_i^j r_i^j(r_{i+1}^j - 2r_i^j + r_{i-1}^j) - p_i^j(r_{i+1}^j - r_{i-1}^j)^2}{4(\Delta x)^2(r_i^j)^2} \quad (9)$$

$$v_i^j = \frac{(q_{i+1}^j - q_{i-1}^j)r_i^j(r_{i+1}^j - r_{i-1}^j) + 4q_i^j r_i^j(r_{i+1}^j - 2r_i^j + r_{i-1}^j) - q_i^j(r_{i+1}^j - r_{i-1}^j)^2}{4(\Delta x)^2(r_i^j)^2} \quad (10)$$

$$r_i^j = p_i^j + q_i^j \quad (11)$$

Here, Δt in equations 5 through 7 refers to total number of time steps and Δx within equations 9 and 10, refers to the total number space intervals. Furthering this, the superscript j represents the current time index and the subscript i represents the current one dimensional space position

for the dependent variable. For example, the term p_i^j would refer to the density of proliferating cells at time j and position i .

2.2 Cellular Conversion Rates and Initial/Boundary Conditions

The functional forms representing the rates of mitosis, quiescence, and necrosis within the model are described by equations 12 - 14 respectively.

$$f(c) = \frac{1 - \tanh(4c - 2)}{2} \quad (12)$$

$$h(c) = \frac{f(c)}{2} \quad (13)$$

$$g(c) = \beta e^{\beta c} \quad (14)$$

These were rates were formulated by Sherratt-Chaplain with the exception of $g(c)$ which follows Gompertz Rule instead due to its more realistic, non-linear, approximation [5]. Beta, β , in equation 14 is another dimensionless parameter similar to that of α and γ that acts as the scaling coefficient for the rate of mitosis. Note that functions $f(c)$ and $h(c)$ are considered to be decreasing functions, as they do not contribute to the proliferating cell density whereas $g(c)$ is increasing under the same pretense. It is also assumed that the rate of quiescence is greater than that of the rate of necrosis such that $f(c) > h(c)$.

Furthermore, at time $t = 0$, the initial conditions are defined as $q(x, 0) = n(x, 0) = 0$, $c(x, 0) = 1$, and the proliferating cell density decreases exponentially as x increases such that $p(x, 0) = e^{-0.1x}$. The boundary conditions at $x = 0$ and as $x \rightarrow \infty$ are:

$$\frac{\partial p}{\partial x} = \frac{\partial q}{\partial x} = 0$$

These boundary conditions ensure the curves approach zero at both extremes. Note that x cannot go to infinity due to computational limits and thus x -values were set to be sufficiently large in the simulations.

2.3 Simulation

Equations 5 through 14 are defined in MATLAB with the initial and boundary conditions detailed above to simulate avascular tumour growth. For the sake of space, the series of data being shared is strictly based on $\alpha = 0.9$, $\beta = 0.5$, and $\gamma = 10$ as these parameter values were found to be best at reflecting experimental trials [6]; showing the most credible results. The MATLAB program used for these simulations can be found in Appendix A with special thanks to Keng-Cheng Ang for providing the preliminary code outline [7]. The resulting plots can be seen in **Figures 4** and **5** below.

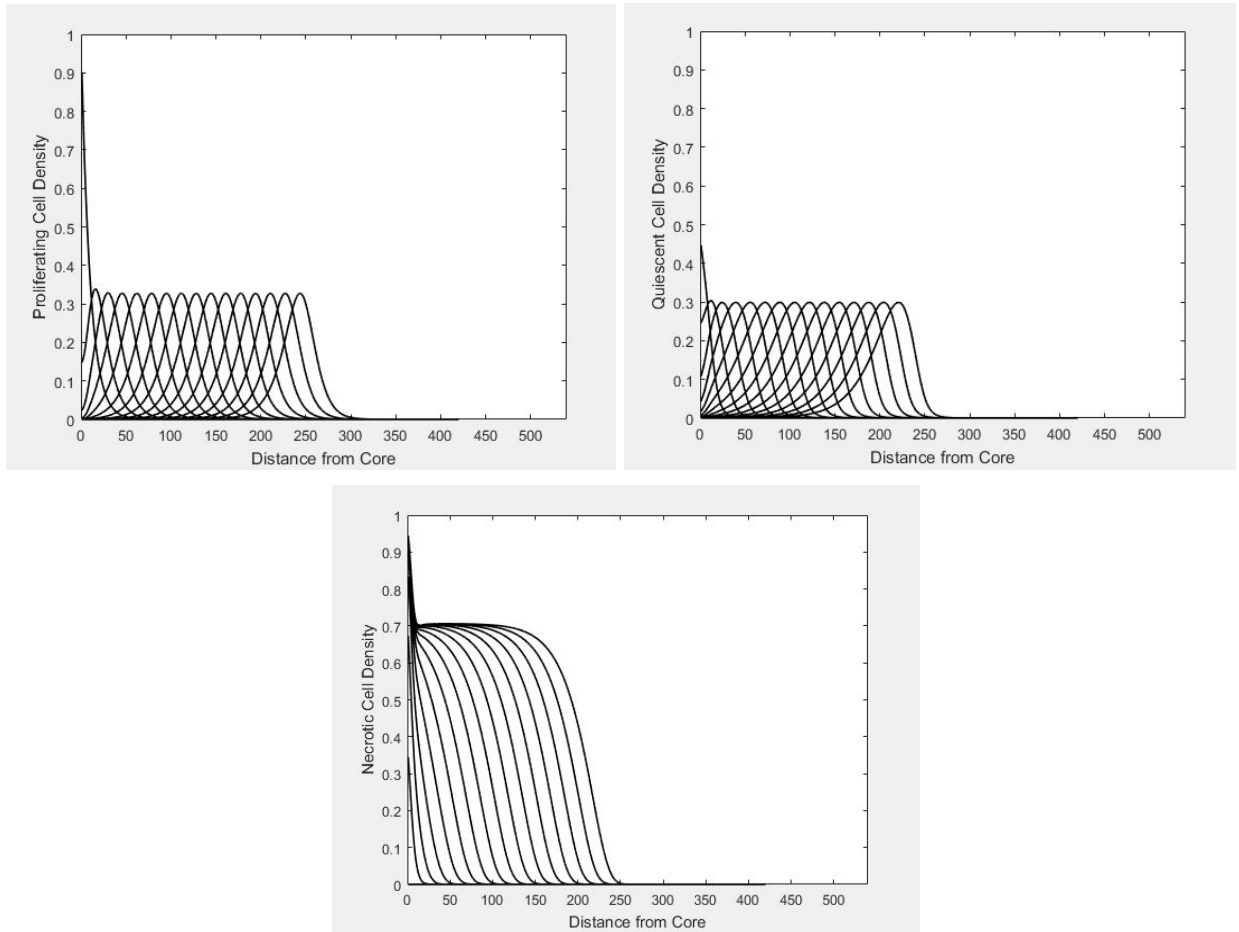


Figure 4: Cell Density Plots for Proliferating, Quiescent, and Necrotic cell populations in regards to a one dimensional space position. The family of curves seen on each plot are in regards to increasing time frames, from left to right, at times $t = 0, 2, 4, \dots, 32$

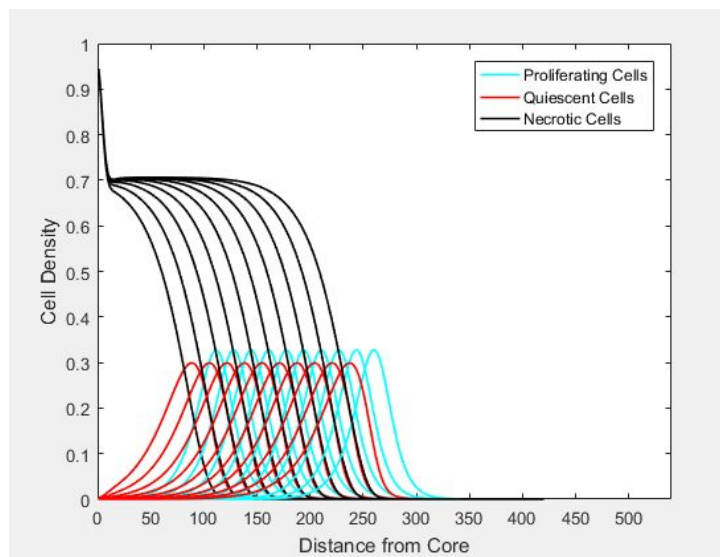


Figure 5: Superimposed Cell Density Plots from times $t = 15, 16, 18, \dots, 32$

Observing the plots, it is clear that a greater population of proliferating cells exist on the tumours exterior followed by a corresponding population of quiescent cells. As time progresses, a growing necrotic core is also seen to be developing within the tumour which matches the three layer depiction of an avascular tumour in **Figure 1**. What is also seen here is pure expansion of the tumour with no regression as there is no loss in nutrient levels nor any therapy applied.

Assuming radial symmetry, the positive number lines of the cell densities can form images of the tumour in 2D or even 3D space at any time t . To do so, a value is set in relation to each of the cell densities at coordinate x to represent the number of cells. This value then dictates the number of points to plot which are then randomly distributed using the MATLAB `rand()` function on the circumference of a circle of radius x at an angle θ between 0 and 2π . This is repeated for each time interval and an example set of images can be seen in **Figure 6**.

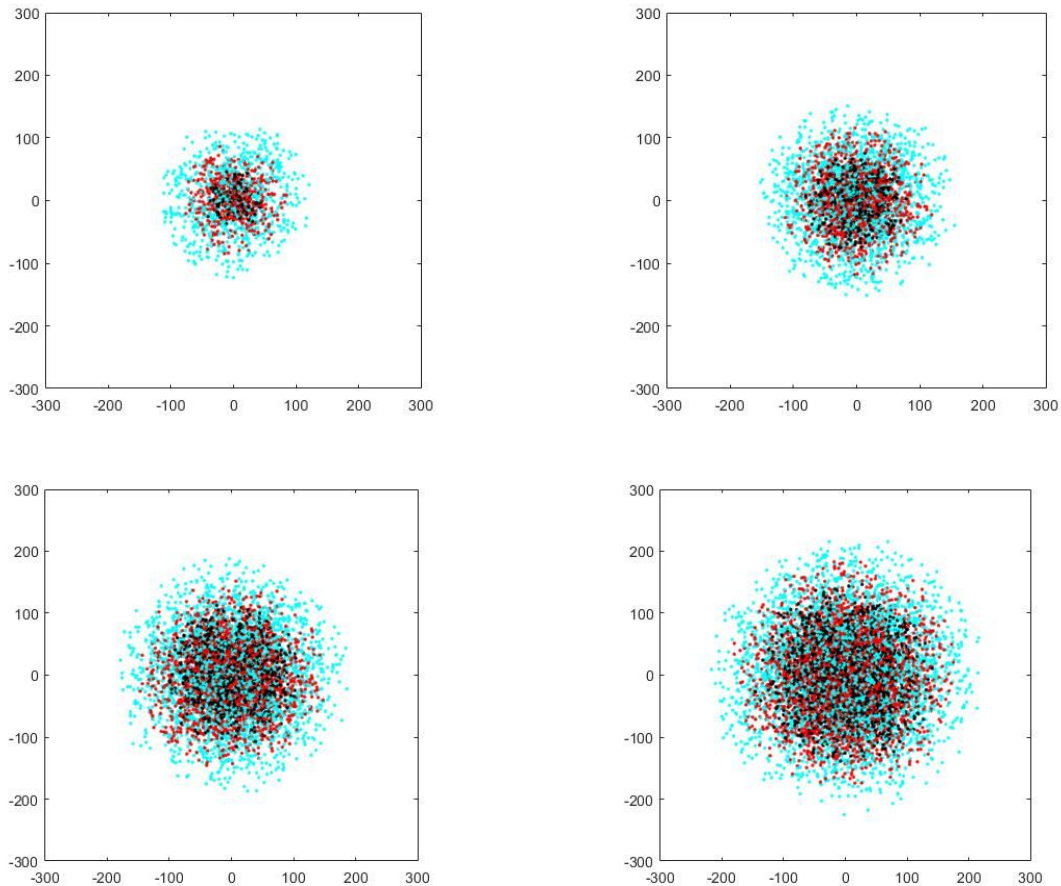


Figure 6: 2D images of simulated avascular tumour growth at time $t = 8, 16, 24,$ and 32 with cyan representing proliferating, red as quiescent, and black as necrotic cells .

These 2D images further support what is observed in the plots with the three layers of proliferating, followed by quiescent, then necrotic cells as time progresses. The program

provided in Appendix A overlays these images on one another; forming an animation of avascular tumour growth.

3 Novel Extension: Chemotherapy

With the model now clearly defined, the extension applied is treatment in the form of chemotherapy. As noted before, the tumour is very small at this point, at roughly 1.4mm, and the typical removal method via surgery is not realistic nor cost efficient. As a result, chemotherapy is generally used as an alternative treatment. Chemotherapy is a type of drug that targets rapidly dividing cells (i.e. proliferating cells) and is applied in numerous ways [8]. The goal of the therapy is to stop the expansion of cancer cells, however, it is considered as a systemic therapy in that it eventually impacts the entire body. This results in side effects including, but not limited to, the destruction of blood cells, platelets, hair follicles, and even the stomach lining [9]. Despite this, it is evidently one of the best treatments methods available and is thus important to integrate into tumour analysis. To introduce chemotherapy into the model, three main cases were considered.

3.1 Case A - Ideal

The ideal case is based off introducing the dosage coefficient, ξ , to directly impede proliferating cell density [9]. This extension is shown here as ' $-\xi p$ ' in equation 1.1. Note that the ξ parameter is between 0 and 1 inclusive in regards to dosage intensity whereby 1 is the strongest dosage possible.

$$\frac{dp}{dt} = \frac{\partial}{\partial x} \left(\frac{p}{p+q} \frac{\partial(p+q)}{\partial x} \right) + g(c)p(1-p-q-n) - f(c)p - \xi p \quad (1.1)$$

3.2 Case B - Probabilistic

However, due to the simplicity of Case A's assumption of direct impedance, it was highly unrealistic. Thus, Case A was further expanded to incorporate proliferating cell survival rate as a function of the dosage coefficient, noted here as equation 15 [10]. The α and β terms are in reference to the same dimensionless radiobiological parameters defined previously.

$$\frac{dp}{dt} = \frac{\partial}{\partial x} \left(\frac{p}{p+q} \frac{\partial(p+q)}{\partial x} \right) + g(c)p(1-p-q-n) - f(c)p - s(\xi) \quad (1.2)$$

$$s(\xi) = e^{-(\alpha\xi + \beta\xi^2)} \quad (15)$$

3.3 Case C - Dormancy

The final Case, C, again expands on Case B in that it also considers the dormancy of quiescent cells. As mentioned, quiescent cells are capable of becoming active dividing cells again given sufficient amount of nutrients, however the original reduced model considered such occurrences to be negligible as the tumour continued to rapidly expand. For real-world behaviour, Case C accounts for these events in addition to the probabilistic behaviour of Case B. A new model diagram was designed and is shown in **Figure 7**, where chemotherapy is formally defined as only affecting the proliferating cells and the quiescence reaction $f(c)$ is now reversible.

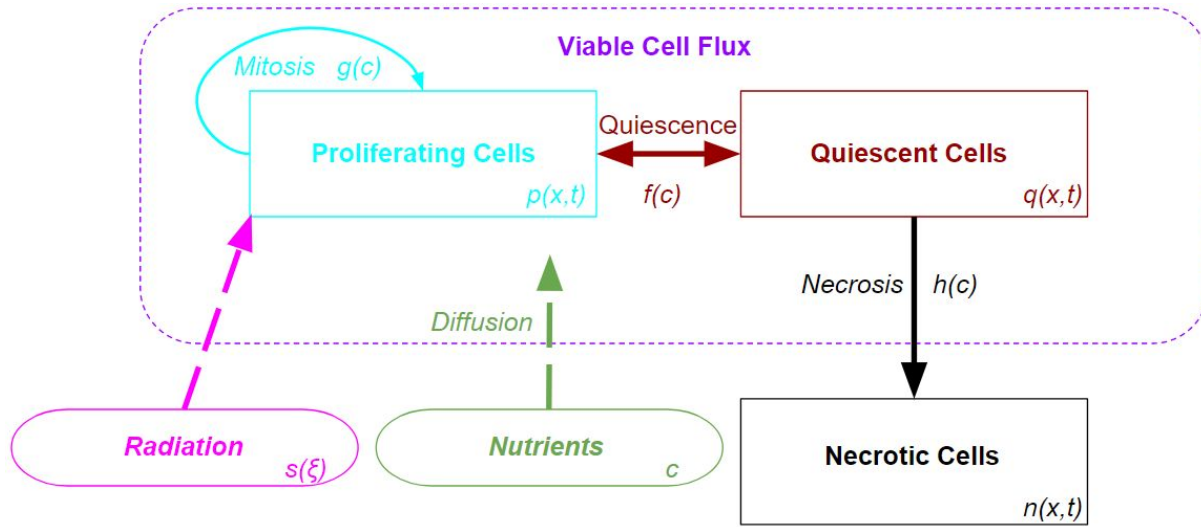


Figure 7: New Avascular Tumour Growth Diagram with Irradiation from Chemotherapy

From this new diagram, the ' $f(c)q$ ' terms were added to equations 1.3 and 2.1 below.

$$\frac{dp}{dt} = \frac{\partial}{\partial x} \left(\frac{p}{p+q} \frac{\partial(p+q)}{\partial x} \right) + g(c)p(1-p-q-n) + f(c)q - f(c)p - s(\xi) \quad (1.3)$$

$$\frac{dq}{dt} = \frac{\partial}{\partial x} \left(\frac{q}{p+q} \frac{\partial(p+q)}{\partial x} \right) + f(c)p - f(c)q - h(c)q \quad (2.1)$$

$$s(\xi) = e^{-(\alpha\xi + \beta\xi^2)} \quad (15)$$

Note that an assumption was made whereby equations 1.3 and 2.1 are only applicable when the proliferating cell density is less than or equal to that of the quiescent cell density within the same time frame.

3.4 Findings

For the sake of space, the plots and images provided here are that of a hyperbolic dosage of 1 to maximize visibility of the impact. All other parameters were maintained at the same value for consistency. The following plots shown in **Figure 8** are generated from treatments A through C as time progresses. Note that these plots only consider two time-steps prior to treatment being applied.

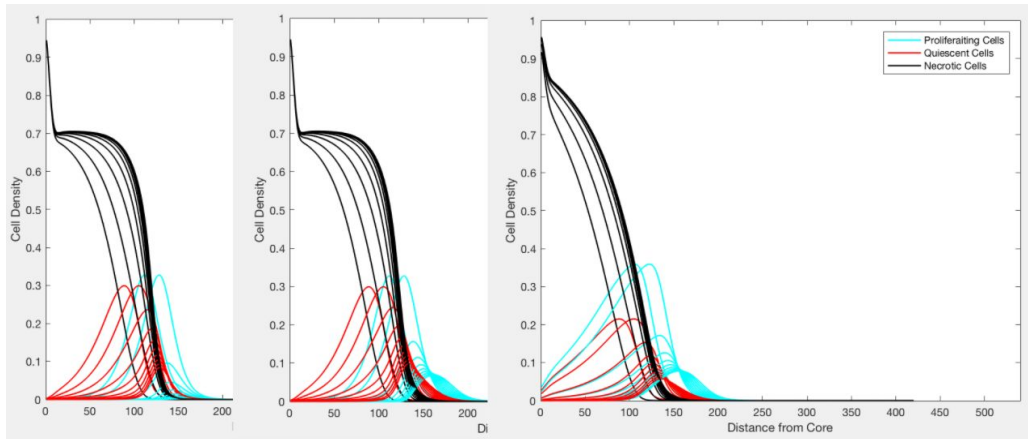


Figure 8: Cell Density Plots of Case A, B, and C respectively from times $t = 15, 16, 18, \dots, 32$

As with the original, these cell density graphs were further illustrated as 2D images, as shown in **Figure 9**, for better analysis.

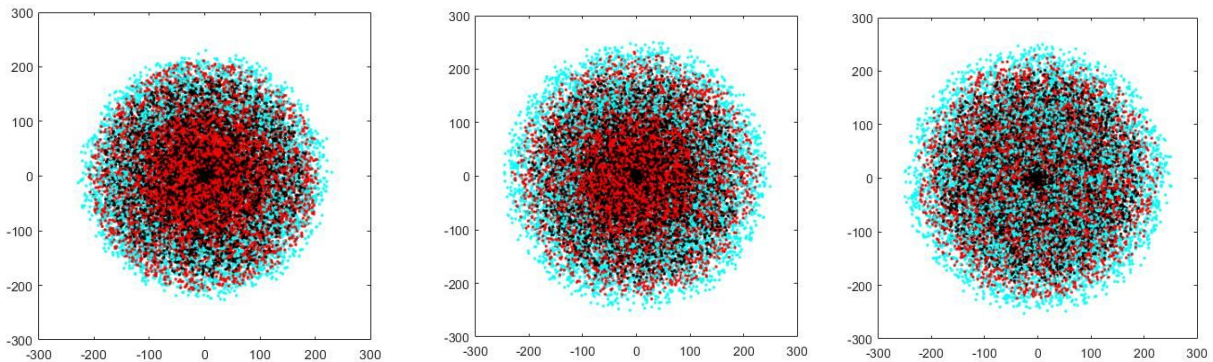


Figure 9: 2D images of simulated avascular tumour growth undergoing treatment A, B, and C respectively at time $t = 64$.

It is observed that after $t = 16$, there is a drastic decrease in cellular density and the transitions to successive curves on the right are much less pronounced. There is also no regression of the tumour as the growth has only been stunted by the irradiation. Additionally, it can be seen that the amount of proliferating cells increases with each successive case, which corresponds to the introduction of the probability term as well as the reversible quiescence

reaction. Furthermore, the cell density slopes are much more gradual in Case C, demonstrating the conversion of proliferating to quiescent and vice versa both before, and during treatment.

To elaborate, in case A, there is near instantaneous proliferation death which results in a high density of both quiescent and necrotic cells and a thin layer of proliferating cells in comparison to that of the other cases. Following this, in Case B, there is a slightly thicker layer of proliferating cells, which accounts for the probabilistic behaviour, however there is still a very high density of quiescent cells. Finally, in case C, there is both the greatest amount of proliferating and lowest amount of quiescent cells which will greatly increase the effectiveness of the treatment. In particular, as quiescent cells are reverted back to a proliferative state, which accounts for the lower quiescent cell count, the applied treatment was able to destroy them as well as the already proliferative cells; resulting in a much higher necrotic density overall.

4 Limitations

The main limitations in regards to Case C were the assumptions that had to be made. It was first assumed that the rate of reverse quiescence was the same as forward quiescence in the original model. Also, the assumption of reverse quiescence only occurring when proliferation cell density is equal to, or less than, the quiescent cell density is simply a rough estimation. Neither assumptions have any experimental findings backing their usage.

Moreover, avascular tumours are very small and the likeliness of using this treatment directly on a tumour is rare, not to mention the difficulty of identifying a tumour so small. However, it is possible that this treatment could be considered for early metastases growth after the original tumour has been removed. It should be noted that such a situation could vary from what has been done in this paper, such as changes in nutrient flow, as the model only assumes the conditions of a brand new and singular forming tumour within a natural body. Likewise, avascularity means that the models and methods explored here cannot be applied to later stages of vascular tumour growth.

Another limitation is the fact that chemotherapy directly impedes only proliferating cells and not quiescent cells, so the one time dosage shown in the findings is not sufficient to completely stunt the tumour and growth would be possible once treatment has ended. The dosage intensity value of 1, through effective in treating the tumour, can also be considered to be fatal for the patient as it would not only affect the tumour but all healthy cells as well. The side effects on the body were not measured in the model simulations but should be held in high regards in determining the best dosage coefficient and frequency of treatment.

5 Plausible Benefits

Despite such limitations however, there are still many plausible benefits that could arise from the results found in this paper. The most important benefit being that of optimizing treatment rate and dosage. Currently, the general treatment regimen for tumours is based on an empirical method, that is, it's based on observation rather than experimental data. Instead, by modelling tumour growth under specific dosages at particular frequencies, a refined

medicinal regime could be derived as to minimize the physical symptoms of irradiation; saving resources and increasing the overall quality of life for all parties.

Beyond this, being able to model and visualize the growth patterns in MATLAB allows for additional experimental study into tumour behavior without the necessity for live growth. This suggests that experiments could be run in a matter of minutes rather than over weeks or months; cutting costs and reducing the associated risk of incubating cancerous diseases. Mathematical models could be the answer for truly understanding cancer in a timely fashion without the need for extensive funding.

6 Conclusion

This paper explored avascular tumour growth as described by the Sherratt-Chaplain reduced model. The model equations are solved with finite differencing and modeled in MATLAB to explore various quantitative results in the form of cell density graphs and tumour growth images assuming radial symmetry.

The novel extension implemented onto the growth model was the effects of irradiation via method of chemotherapy. Three different cases were considered, each expanding upon the last in terms of modelling realism. The irradiation clauses all stunted tumour growth at various rates as expected, with the ability to explore such rates at different dosage levels.

The limitations of the model and the irradiation methods were considered and the benefits of using MATLAB to model were considered. Clinical implementation was also explored after irradiation cases showed time frames that can be worked with.

7 References

- [1]"Types of tumours - Canadian Cancer Society", www.cancer.ca, 2018. [Online]. Available: <http://www.cancer.ca/en/cancer-information/cancer-101/what-is-cancer/types-of-tumours/?registration=on>. [Accessed: 01- Apr- 2018].
- [2] J. Adam, "A Simplified Mathematical Model of Tumor Growth", *Mathematical Biosciences*, vol. 81, no. 2, pp. 229-244, 1986.
- [3]H. Greenspan, "Models for the Growth of a Solid Tumor by Diffusion", *Studies in Applied Mathematics*, vol. 51, no. 4, pp. 317-340, 1972.
- [4] J. Sherratt and M. Chaplain, "A New Mathematical Model for Avascular Tumour Growth", *Journal of Mathematical Biology*, vol. 43, no. 4, pp. 291-312, 2001.
- [5]Nirmala, C., Rao, J. A., Ruifrok, A. C., Langford, L. A. and Obeyesekere, M., "Growth characteristics of glioblastoma spheroids", *International Journal of Oncology*, 2001, 19, 1109-1115.
- [6] T. Soon and A. Cheng, "A Numerical Simulation of Avascular Tumour Growth", *ANZIAM Journal*, vol. 46, pp. 902-917, 2005.
- [7] K.C Ang, "Analysis of a Tumour Growth Model with MATLAB", *Proceedings of the 14th Asian Technology Conference in Mathematics*, Beijing, China, 2009.
- [8]"Learn About Managing Your Chemotherapy", *chemotherapy*, 2018. [Online]. Available: http://www.chemotherapy.com/new_to_chemo/what_is_chemo/. [Accessed: 01- Apr- 2018]
- [9]H. Enderling and M. Chaplain, "Mathematical Modeling of Tumor Growth and Treatment", *Current Pharmaceutical Design*, vol. 20, no. 30, pp. 4934-4940, 2014.
- [10]E. Zacharaki, G. Stamatakos, K. Nikita and N. Uzunoglu, "Simulating growth dynamics and radiation response of avascular tumour spheroids—model validation in the case of an EMT6/Ro multicellular spheroid", *Computer Methods and Programs in Biomedicine*, vol. 76, no. 3, pp. 193-206, 2004.

8 Appendix A

The code used for each of the simulations can be found below. Note that this was run on Matlab 2016a and may need to be altered for different versions. Instructions are included as comments within the code.

```
classdef TumourGrowth < handle
    % Avascular tumour growth with radial symmetry as adapted
    % from the Sherratt-Chaplain model. It accounts for cell motility in
    % both proliferating and quiescent cellular layers along with cell
    % necrosis. Treatment is applied halfway through the simulation if
    % applicable

    %Instructions:
    %Save code as 'TumourGrowth.m'
    %Change MATLAB directory to 'TumourGrowth.m' save location
    %Run 'x = TumourGrowth()' to initialize object
    %Run 'x.simulate(0)' for Untreated growth
    %Run 'x.simulate(1)' for Ideal Treatment growth
    %Run 'x.simulate(2)' for Probabilistic Treatment growth
    %Run 'x.simulate(3)' for Realistic Treatment growth

    properties (Access = public)
        alpha = 0.9; %buffer between cells and nutrients - between 0.1 and 1
        beta = 0.5; %rate coefficient for mitosis - between 0.1 and 1
        gamma = 10; %in vivo conditions surrounding cells - greater than proliferating density
        dx = 1; %maximum step size in spatial coordinate
        X = 420; %spacial coordinate boundary
        Nx; %Total step count for spatial axes
        dt = 0.004; %maximum step size in time
        T = 16; %total tumour growth time
        Nt; %Total step count for time index
        c0 = 1; %initial nutrient count - between 0 and 1
        xi = 1; %irradiation level - between 0 and 1
        animationSteps= 125; %Resolution of 64
        %Change animationSteps as appropriate. The lower the number, the higher
        %the resolution but the more intensive the simulation:
        %16/(2*0.250) = 32 vs. 16/(2*0.125) = 64 vs. 16/(2*0.0005) = 1600
    end

    methods (Static)
        function result = f(c)
```

```

    %Determines rate of quiescence based off current nutrient value
    result = 0.5*(1-tanh(4*c-2));
end
end

methods (Access = public)
function result = h(TG,c)
    %Determines rate of necrosis based off current nutrient value and quiescence
    result = 0.5*TG.f(c);
end

function result = g(TG,c)
    %Determines rate of proliferation based off current nutrient value and beta
    result = TG.beta*exp(TG.beta*c);
end

function simulate(TG, treatment)
    %Initializes all required arrays / values and calls all simulation functions

    x = [TG.dx:TG.dx:TG.X]; %Spatial axes
    TG.Nx = round(TG.X/TG.dx); %Total Spatial Steps
    TG.Nt = 2*round(TG.T/TG.dt); %Total Time - *2 accounts for treatment
    p = zeros(1,TG.Nx); %Proliferating cell count in x-direction
    nextp = zeros(1,TG.Nx);
    q = zeros(1,TG.Nx); %Quiescent cell count in x-direction
    nextq = zeros(1,TG.Nx);
    n = zeros(1,TG.Nx); %Necrotic cell count in x-direction
    nextn = zeros(1,TG.Nx);
    u = zeros(1,TG.Nx); %From forward differencing equations
    v = zeros(1,TG.Nx); %From forward differencing equations
    r = zeros(1,TG.Nx); %To simplify forward differencing equations
    c = zeros(1,TG.Nx); %Nutrient count in x-direction
    P = zeros(TG.Nt,TG.Nx); %Proliferating Cell density at x at t
    Q = zeros(TG.Nt,TG.Nx); %Quiescent Cell density at x at t
    N = zeros(TG.Nt,TG.Nx); %Necrotic Cell density at x at t

    p = exp(-0.1.*x); %Initial Proliferating Cell Density

    %Print selected simulation type
    if treatment == 1
        disp('Ideal Treatment')
    elseif treatment == 2

```



```

    disp('Probability Treatment')
elseif treatment == 3
    disp('Realistic Treatment')
else
    disp('Untreated')
end

%Set initial values for dynamic equations as cell of arrays
fdm = {p; nextp; q; nextq; n; nextn; u; v; r; c};
cellDInit = {P; Q; N};

%Run dynamics
cellID = TG.dynamics(fdm, cellDInit, treatment);

%Plot Growth Figures
TG.plot(cellID);

%Run Animation
TG.animate(cellID);
end

function result = dynamics(TG, fdm, cellDInit, treatment)
    %Run dynamic equations that were derived through forward
    %differencing of Sherratt-Chaplain model. Returns array of
    %cells corresponding to cellular densities

    %Seperate arrays and initial values from passed in data
    p = cell2mat(fdm(1)); nextp = cell2mat(fdm(2));
    q = cell2mat(fdm(3)); nextq = cell2mat(fdm(4));
    n = cell2mat(fdm(5)); nextn = cell2mat(fdm(6));
    u = cell2mat(fdm(7)); v = cell2mat(fdm(8)); r = cell2mat(fdm(9));
    c = cell2mat(fdm(10));
    P = cell2mat(cellDInit(1));
    Q = cell2mat(cellDInit(2));
    N = cell2mat(cellDInit(3));

    for k=1:TG.Nt
        r = p + q;
        c = (TG.c0.*TG.gamma./(TG.gamma+p)).*(1-TG.alpha.*(p+q+n));
        for i=2:TG.Nx-1
            u(i) = ((p(i+1)-p(i-1))*r(i)*(r(i+1)-r(i-1))+ ...
                4*p(i)*r(i)*(r(i+1)-2*r(i)+r(i-1))- ...

```

```

    p(i)*(r(i+1)-r(i-1))^2)/(2*(TG.dx*r(i))^2);
v(i) = ((q(i+1)-q(i-1))*r(i)*(r(i+1)-r(i-1))+ ...
    4*q(i)*r(i)*(r(i+1)-2*r(i)+r(i-1))- ...
    q(i)*(r(i+1)-r(i-1))^2)/(2*(TG.dx*r(i))^2);
end
if k > TG.Nt/2 %Apply Treatment halfway through simulation
    if treatment == 1 %Ideal Treatment (Case A)
        nextp=p+TG.dt.*(u+TG.g(c).*p.*(1-(p+q+n))-TG.f(c).*p-TG.xi*p);
        nextq = q+TG.dt.*(v+TG.f(c).*p-TG.h(c).*q);
    elseif treatment == 2 %Probability Treatment (Case B)
        sprob = p*exp(-TG.alpha*TG.xi + TG.beta*TG.xi^2);
        nextp=p+TG.dt.*(u+TG.g(c).*p.*(1-(p+q+n))-TG.f(c).*p-sprob);
        nextq = q+TG.dt.*(v+TG.f(c).*p-TG.h(c).*q);
    elseif treatment == 3 %Realistic Treatment (Case C)
        sprob = p*exp(-TG.alpha*TG.xi + TG.beta*TG.xi^2);
        if max(P(k,:)) <= max(Q(k,:)) %Set Quiescence as Reversible Reaction
            nextp=p+TG.dt.*(u+TG.g(c).*p.*(1-(p+q+n))-TG.f(c).*p+TG.f(c).*q-sprob);
            nextq=q+TG.dt.*(v+TG.f(c).*p-TG.f(c).*q-TG.h(c).*q);
        else %Keep Quiescence as irreversible until Proliferating cell density lowers
            nextp=p+TG.dt.*(u+TG.g(c).*p.*(1-(p+q+n))-TG.f(c).*p-sprob);
            nextq=q+TG.dt.*(v+TG.f(c).*p-TG.h(c).*q);
        end
    else %Untreated (Original)
        nextp=p+TG.dt.*(u+TG.g(c).*p.*(1-(p+q+n))-TG.f(c).*p);
        nextq = q+TG.dt.*(v+TG.f(c).*p-TG.h(c).*q);
    end
elseif treatment == 3 %Realistic Growth until Treatment 3 begins
    if max(P(k,:)) <= max(Q(k,:))
        nextp=p+TG.dt.*(u+TG.g(c).*p.*(1-(p+q+n))-TG.f(c).*p+TG.f(c).*q);
        nextq=q+TG.dt.*(v+TG.f(c).*p-TG.f(c).*q-TG.h(c).*q);
    else
        nextp=p+TG.dt.*(u+TG.g(c).*p.*(1-(p+q+n))-TG.f(c).*p);
        nextq=q+TG.dt.*(v+TG.f(c).*p-TG.h(c).*q);
    end
else %Original Growth until Treatment 0, 1 or 2 begins
    nextp=p+TG.dt.*(u+TG.g(c).*p.*(1-(p+q+n))-TG.f(c).*p);
    nextq = q+TG.dt.*(v+TG.f(c).*p-TG.h(c).*q);
end
nextn = n+TG.dt.*(TG.h(c).*q);
p = nextp;
q = nextq;
n = nextn;

```

```

    P(k,:) = p;
    Q(k,:) = q;
    N(k,:) = n;
end
result = {P; Q; N};
end

function plot(TG, cellID)
    %Plot all Cell Densities for analysis

    %Seperate Cell Densities from passed in data
    P = cell2mat(cellID(1));
    Q = cell2mat(cellID(2));
    N = cell2mat(cellID(3));

    %Plot Proliferating Cell Density
    figure(1)
    for n=1:500:TG.Nt
        plot(P(n,:), 'k', 'LineWidth', 1.2); hold on;
        ylabel('Proliferating Cell Density')
        xlabel('Distance from Core')
    end
    axis([0 540 0 1]);

    %Plot Quiescent Cell Density
    figure(2)
    for n=1:500:TG.Nt
        plot(Q(n,:), 'k', 'LineWidth', 1.2); hold on;
        ylabel('Quiescent Cell Density')
        xlabel('Distance from Core')
    end
    axis([0 540 0 1]);

    %Plot Necrotic Cell Density
    figure(3)
    for n=1:500:TG.Nt
        plot(N(n,:), 'k', 'LineWidth', 1.2); hold on;
        ylabel('Necrotic Cell Density')
        xlabel('Distance from Core')
    end
    axis([0 540 0 1]);

```

```

%Plot Superimposed Cell Densities (Proliferating, Quiescent and
%Necrotic) from just before treatment to treatment end
figure(4)
for n=3500:500:TG.Nt
    plot(P(n,:), 'c', 'LineWidth', 1.2); hold on;
    plot(Q(n,:), 'r', 'LineWidth', 1.2); hold on;
    plot(N(n,:), 'k', 'LineWidth', 1.2); hold on;
end
ylabel('Cell Density')
xlabel('Distance from Core')
legend('Proliferating Cells', 'Quiescent Cells', 'Necrotic Cells')
axis([0 540 0 1]);
end

function animate(TG, cellID)
    %Run animation (assuming radial symmetry) of growth pattern and
    %save each animation step as an image

    %Seperate Cell Densities from passed in data
    P = cell2mat(cellID(1));
    Q = cell2mat(cellID(2));
    N = cell2mat(cellID(3));

    %Animate
    rand('state', sum(100*clock));
    prefix='t'; %prefix for images
    Nm=0; %keep track of image number
    figure(5)
    for n=1:TG.animationSteps:TG.Nt
        Nm=Nm+1;
        for i=1:TG.Nx
            %Determine number of cells at space i at time n to 4 decimal places and plot
            randomly on radius i
            tP=round(P(n,i),4);
            tQ=round(Q(n,i),4);
            tN=round(N(n,i),4);
            for m=0.0001:tP
                theta=2*pi*rand();
                plot(i*sin(theta), i*cos(theta), 'c. '); hold on;
            end
            for m=0.0001:tQ
                theta=2*pi*rand();

```

```
        plot(i*sin(theta),i*cos(theta),'r. '); hold on;
    end
    for m=0.0001:tN
        theta=2*pi*rand();
        plot(i*sin(theta),i*cos(theta),'k. '); hold on;
    end
    axis square
    axis([-300 300 -300 300])
end
%Save plot as image
print('-djpeg','-r100',sprintf('%s_%s',prefix,num2str(Nm)));
end
end
end
end
```